ELSEVIER

Coastal Engineering 46 (2002) 127–138

Coastal Engineering
An International Journal for Coastal, Harbour and Offshore Engineers

www.elsevier.com/locate/coastaleng

Changes in coastal sediment transport processes due to construction of New Damietta Harbour, Nile Delta, Egypt

Hesham M. El-Asmar [a], Kevin White [b,*]

[a] Department of Geology, Damietta Faculty of Science, Damietta 34517, Egypt
[b] Landscape and Landform Research Group, Department of Geography, The University of Reading, Whiteknights, Reading, RG6 6AB, UK

Received 16 March 2001; received in revised form 24 January 2002; accepted 25 April 2002

Abstract

A combination of remote sensing, field surveys and sedimentological analysis of beach sands is used to assess changes of the shorelines consequent to the construction of a harbour at Damietta on the Nile Delta. The results indicate that harbour construction, and, in particular, the construction of two jetties that extend out from the harbour entrance, have created a discontinuity in the eastward-moving littoral drift. Imagery from Landsat Thematic Mapper provides crude assessments of the rate of up-drift accretion and down-drift erosion of the shorelines, despite the relatively coarse pixel size (30 m) and short time-scale of the monitoring period (1984–1987–1991). Conventional bathymetric surveys highlight changes in the nearshore environment associated with the growth of the updrift accretionary wedge and siltation of the harbour access channel. Beach sediments also provide a record of the changes in erosion and accretion-dominated process domains on both sides of the harbour entrance. The accretionary beaches west of the western jetty having a finer mean grain size with a tendency to poorer sorting skewed to the finer fraction and preferential increase in the assemblage of low-density non-opaque heavy minerals. The beach sands of the erosional shoreline east of the eastern jetty are characterised by coarser mean grain size with a tendency to better sorting skewed to the coarser fraction and heavy mineral assemblages dominated by opaques and high-density non-opaques. The synergistic use of remote sensing, bathymetric surveying and sedimentology provides evidence that changes have affected a much larger area than predicted at the time of harbour construction. © 2002 Elsevier Science B.V. All rights reserved.

Keywords: Nile Delta; Remote sensing; Coastal erosion; Sedimentology

1. Introduction

The Aswan High Dam, completed in 1964, was built to control the flow of the Nile, to generate electricity and to provide water for irrigation. However, the dam has also impacted the sediment flux; amounts of sediment reaching the river mouths at Rosetta and Damietta are no longer sufficient to nourish the Nile Delta coastline and prevent coastal erosion (Lotfy and Frihy, 1993; Stanley, 1996). As a result, a great deal of effort has been expended on construction of coastal defence structures to protect sections of the coast of particular socioeconomic importance, such as resort beaches, new communities and harbours. Due in part to the absence of a unified strategy for protecting the Nile Delta coast as a whole, contemporary erosion of the coastline threatens to

* Corresponding author. Fax: +44-1734-755865.
E-mail address: k.h.white@reading.ac.uk (K. White).

0378-3839/02/$ - see front matter © 2002 Elsevier Science B.V. All rights reserved.
PII: S0378-3839(02)00068-6

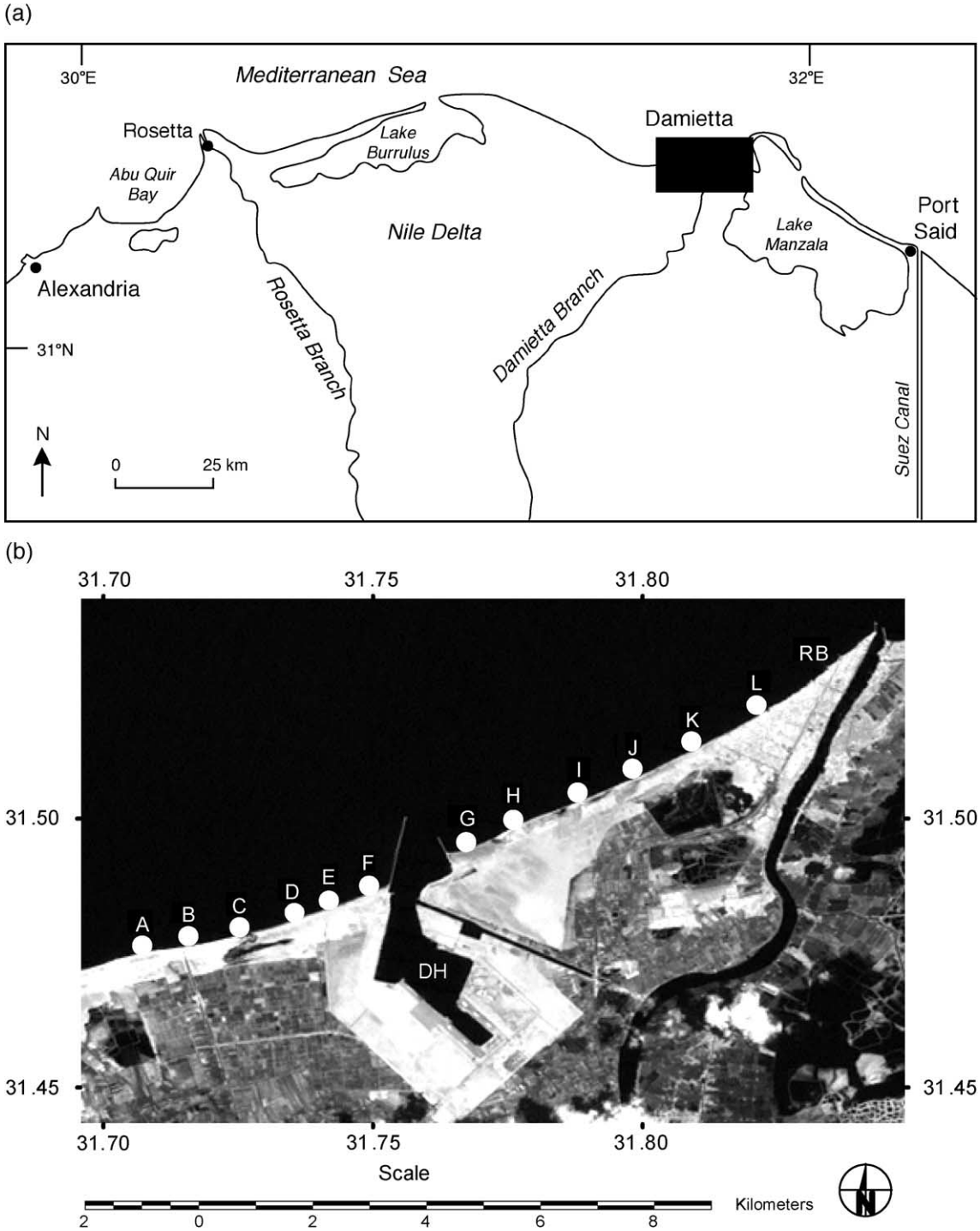

Fig. 1. Location map of Damietta Harbour (a), showing transect points mentioned in the text (b). RB = Ras El-Bar.

become a major environmental hazard (White and El-Asmar, 1999).

In the early 1980s, a decision was made to construct a new harbour and city to the northwest of Damietta (Fig. 1) in order to increase the trade potential along the Mediterranean coast. It was also decided to construct the harbour some distance inland in order to protect it from winter storms so that it could be used year-round and avoid shipping delays. A location was selected in a coastal embayment with minimal effects from waves and currents (Sogreah, 1982). The location was described by UNESCO/UNDP (1978) as one of long-term coastal accretion and convergence of littoral drift, which is supported by a significant field of active sand dunes fed by material derived from this section of beach (Frihy et al., 1991; Fanos, 1995). The harbour is composed of two parts: the shipping area, which is an inland basin containing 12 platforms, and an access channel connecting the shipping area with the Mediterranean Sea. Some 5 million m^3 of sediment was dredged during the excavation of the harbour entrance and placed along the eastern (downdrift) coast adjacent to the harbour (Frihy et al., 1991). In 1982, the entrance to the access channel was protected against littoral drift by the construction of two jetties, which were extended in 1985. The western jetty is 1300 m long and the eastern jetty is 600 m long.

Wave action along the Nile Delta coast is seasonal with high storm waves approaching from the NW–NNW during the winter (October to March). These generate eastward longshore currents with velocities of up to 0.9 m s^{-1} (Tetra Tech., 1984), driving a sediment flux. Swells during the spring and summer are predominantly from NNW–WNW, with a small component from NNE. These can cause either easterly or westerly sediment transport depending on local shoreline orientation. Wave climatology data were collected from 1985 to 1990 at Abu-Quir, east of Alexandria (Fig. 1(a)), and Ras El-Bar (Fig. 1(b)); the modal significant wave height for both stations is 0.75 m and significant wave period is 7–8 s during winter decreasing to 5 s in summer (Nafaa, 1995). The Mediterranean Sea at the Nile Delta has an extremely low tidal range; measurements at the inlet to Lake Burrulus show a mean tidal range (change in the level of the sea during one tidal day—approximately 25 h) of only 14 cm over the last 20 years (El-Fishawi, 1994), with 60-cm variation in daily mean sea level at Port Said over the period 1980–1986 (Eid et al., 1997).

Several estimates of the magnitude of littoral drift have been made for this section of coast before the harbour was built. Sogreah (1982) estimates a drift of some 0.66 million m^3 $year^{-1}$ to the east and 0.26 million m^3 $year^{-1}$ to the west, resulting in a net annual transport of 0.4 million m^3 $year^{-1}$ to the east. Other estimates of net transport include 1.16 million m^3 $year^{-1}$ (Kadib, 1969), 0.8 million m^3 $year^{-1}$ (Tetra Tech., 1984) and 0.6–1.8 million m^3 $year^{-1}$ (A.S.R.T., 1988).

After construction of the harbour, the resultant eastward sediment flux was reduced almost to zero in the vicinity of the harbour entrance. The effect of the net sand deficit (somewhere between 0.4 million and 1.8 million m^3 $year^{-1}$, Sogreah, 1982; Kadib, 1969; Tetra Tech., 1984; A.S.R.T., 1988) is already apparent adjacent to the harbour entrance. Accretion against the western jetty has resulted in seaward advance of the shoreline of some 125 m between 1981 and 1993, an average of 10.4 m $year^{-1}$ (El-Asmar, 1995). Erosion along the eastern jetty has resulted in 80 m of landward recession of the shoreline between 1984 and 1993, an average shoreline retreat of 8.9 m $year^{-1}$ (El-Asmar, 1995). However, the wider impact of these changes on the coastal sediment transport system is unknown due to the effort required to extend detailed field surveys further along the coast. Ongoing research seeks to apply analytical solutions to this classical case of shoreline response to the introduction of a littoral barrier in the presence of net longshore sediment transport. However, this paper presents a methodology to determine the spatial extent of the impact of coastline changes using a combination of remote sensing, nearshore bathymetric surveys and sedimentology. These data will be used to validate the output of analytical models when these become available.

2. Methodology

The synoptic overview provided by satellite remote sensing, along with the capability for repeat coverage, enables changes in the landscape to be seen at a broader scale and provides a spatial context within

which to evaluate the significance of detailed field data (Millington and Townshend, 1987). Landsat Thematic Mapper data (path 176 row 38) of the eastern Nile Delta coast were acquired for three dates (03/08/1984, 11/07/1987 and 04/08/1991). The 1991 scene was registered to geographical coordinates using a second order polynomial to transform the line and column locations of pixels to their latitude and longitude locations derived from map and GPS data. The 1984 and 1987 images were then registered to the geocorrected 1991 scene using second order polynomials. The root mean square error of the transformation was not permitted to exceed 0.55 pixel (or 0.4 pixel for image-to-image registration). Full details of the ground control points and assessment of the accuracy of the transformations are given elsewhere (El-Asmar and White, 1997).

In order to delineate the land/sea boundary, Thematic Mapper band 7 (shortwave infrared) was used. Shorter wavelengths allow some penetration through water, giving a more gradational effect and making exact delineation of the coastline difficult (Wilson, 1997). Problems of high reflectance offshore due to surf in the breaker zone are also ameliorated by using shortwave infrared data (Frouin et al., 1996).

Image segmentation and edge detection algorithms, developed for robot vision, follow the process of human image interpretation (Cross et al., 1988) by dividing an image into different regions (Sonka et al., 1993). There are two techniques: the edge detection (disjunctive) approach finds and links high frequency edges around regions by passing spatial convolution filters over the image. The alternative (conjunctive) approach seeks to grow homogeneous regions by merging pixels or subregions on the basis of some similarity criterion (Lemoigne and Tilton, 1995). The latter, region-growing approach has been found to be more suitable for most remote sensing applications (Kettig and Landgrebe, 1976) and is adopted here. For segmentation of different land cover types, such as agricultural land use, various measurements of texture are normally necessary (Weszka et al., 1976; Chen and Pavlidis, 1979). However, segmentation of land and sea in shortwave infrared optical images can usually be implemented simply by using a specified grey level difference from the region mean as a homogeneity criterion by virtue of their distinct spectral reflectance characteristics at these wavelengths. In this project, mean and standard deviation statistics of beach surfaces and sea surfaces were extracted from the georeferenced imagery and used to specify the homogeneity criterion.

Little preprocessing is necessary for automatic segmentation of water (Wilson, 1997). In order to ensure that the same homogeneity criterion could be applied to all images, a cosine correction was applied for differences in sun angle arising from the different times of the year that the images were collected. This only had a minimal effect on DN values (digital number—a measure of received radiance for each pixel), as all images were acquired in the Northern Hemisphere summer months of July and August. A DN difference from region mean of 20 was found to account for variability in the sea reflectance in Thematic Mapper band 7, while still ensuring that the coast was always identified as a region boundary. The region mean was updated with each additional merge. Region growing was initiated at the same point over the sea for each date in order to avoid differences arising from merging order. Cloud regions over the sea were deleted and interior shorelines of Lakes Burrulus and Manzala, picked up as the region growth extended down canals and drainage channels, were deleted manually to leave only the coastline. The resulting vectors are located at intercell, rather than on-cell boundaries (Fleck, 1992), forming a crack-edge representation of the coastline of the Nile Delta at the time of image acquisition. Standard GIS measurement tools are used to determine the distance the shoreline has moved between image acquisitions. These measurements enable calculation of rates of shoreline retreat or advance. Changes in the rates of shoreline movement in the two periods between the three image acquisitions are used to determine whether shoreline movement is accelerating (movement 1984–1987 < 1987–1991) or decelerating (movement 1984–1987 > 1987–1991). Measurements were taken at 12 sections normal to the shoreline and covering a distance of about 10.4 km, the locations of which are shown in Fig. 1(b). Six of these (sections A–F) are west of the western jetty and six (sections G–L) to the east of the eastern jetty.

The instantaneous field of view of Thematic Mapper data is 30 m (Forshaw et al., 1983). This is resampled to 28.5 m in the standard NASA format used here (Townshend et al., 1988), although it should be noted that this does not improve the actual spatial

resolution of the data (Townshend, 1980). Thus, the position of the crack edge can only be defined to 30-m precision. To avoid problems of unjustified precision of data, all measurements used herein are quantised to 30 m, representing the instantaneous field of view of the instrument.

Sediment characteristics can also be used to recognise the dominant process domains at a location on a coastline. Samples of beach-face sediments were collected at sampling points A to L (Fig. 1(b)). Three samples were collected at each location, one at the low water mark, one at the high water mark and one midway between these two. These were dry-sieved into phi particle size classes to determine the particle size distribution. Heavy mineral separation was carried out on the very fine sand fraction (0.125–0.063 mm) in order to calculate the percentage of total heavy minerals (weight of heavy minerals/weight of very fine sand fraction)/100. Heavy minerals were identified using polarised microscopy.

3. Results and discussion

3.1. Shoreline change detection, remote sensing and bathymetry

The remotely sensed shoreline change detection results (Table 1) indicate that significant shoreline advance extends a considerable distance west of the western jetty (Fig. 2a), and significant shoreline recession extends a considerable distance east of the eastern jetty (Fig. 2b). These results are currently being used to validate hydrodynamic modelling of sediment transport around the harbour.

3.1.1. Zone of accretion

The zone of accretion (sections A to F, Fig. 1 and Table 1) extends west of the western jetty for some 4.2 km towards New Damietta City. Prior to construction of the harbour, the shoreline was stable (Sogreah, 1982). However, following completion of harbour construction, the shoreline advanced seaward at a rate of 25 m year^{-1} between 1983 and 1993, measured using conventional field surveying techniques (El-Asmar, 1995). This rate is very close to the estimate from the remote sensing technique (up to 21 m year^{-1} between 1984 and 1991, Table 1), providing some confidence in our estimates.

Changes in the sediment flux brought about by construction of the two jetties along the harbour also resulted in other changes in the foreshore environment, which cannot be remotely sensed, but require detailed field surveys to ascertain. The available bathymetric data for the accretionary segment (sections A–F) west of the western jetty show that depth contours of 1991and 1997 are prograding seaward in a similar fashion to the shoreline itself (Fig. 3). Note that the shoreline appears more convoluted when surveyed in the field (Fig. 3) than when mapped from the Landsat Thematic Mapper imagery (Fig. 2a) due to the 30-m pixel size of the remotely sensed image.

Table 1
Changes in shoreline position and rates of changes at 12 locations along the coast on either side of Damietta Harbour

Coastline Segment	Section	Change 1984–1987 (m)	Rate of change 1984–1987 (m year^{-1})	Change 1987–1991 (m)	Rate of change 1987–1991 (m year^{-1})	Total change 1984–1991 (m)	Rate of change 1984–1991 (m year^{-1})
Accretionary segment west of the western jetty	A	0	0	0	0	0	0
	B	+30	+10	+30	+8	+60	+9
	C	+30	+10	+30	+8	+60	+9
	D	+90	+30	+60	+15	+150	+21
	E	+60	+20	+60	+15	+120	+17
	F	+60	+20	+60	+15	+120	+17
Erosional segment east of the eastern jetty	G	0	0	−60	−15	−60	−9
	H	+270	+90	−90	−23	+180	+26
	I	−120	−40	−60	−15	−180	−26
	J	+60	+20	0	0	+60	+9
	K	+30	+10	0	0	+30	+4
	L	0	0	0	0	0	0

Positive values indicate seaward progradation of coastline, negative values indicate landward retreat of shoreline.

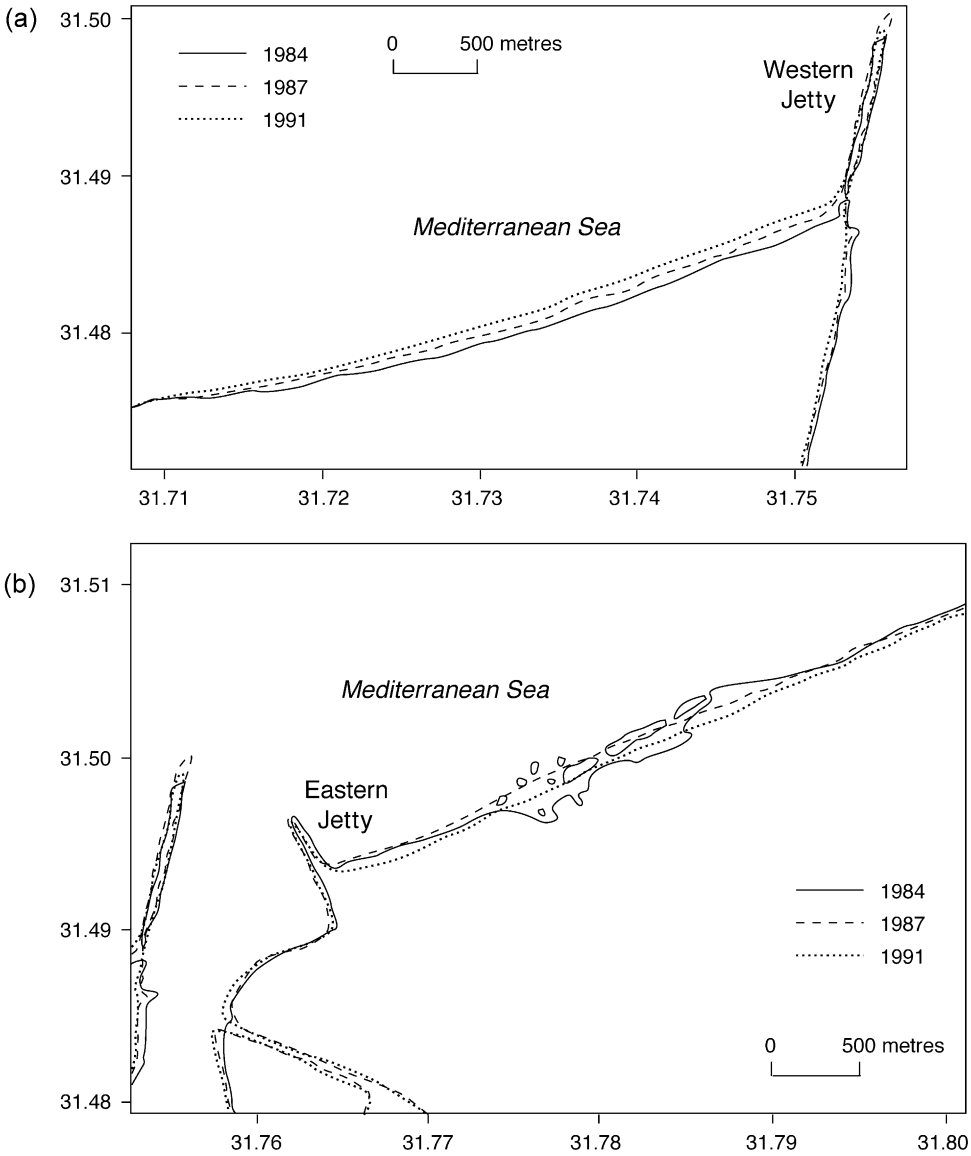

Fig. 2. Vector maps showing the changes in shoreline position to the (a) west and (b) east of Damietta Harbour, produced by automatic segmentation of Landsat Thematic Mapper imagery. Shoreline positions are mapped at 1984, 1998 and 1991.

3.1.2. Zone of erosion

The temporal pattern of erosion and accretion is more complex east of the eastern jetty. Although this part of the shoreline is experiencing erosion due to interruption of littoral drift from 1987 to 1991 especially at sections G, H and I (Fig. 1 and Table 1), a complex pattern of both accretion and erosion is recorded at sections H, I, J and K from 1984 to 1987 (Table 1). The apparent shoreline advance recorded at sections H, J and K is due to the placement of some 5 million m^3 of sediment dredged during the excavation of the harbour entrance (Frihy et al., 1991). The redistribution of this material, both along-shore and offshore during the following 7 years accounts for the apparent shoreline advance during this period. Sogreah (1982) had predicted erosion to

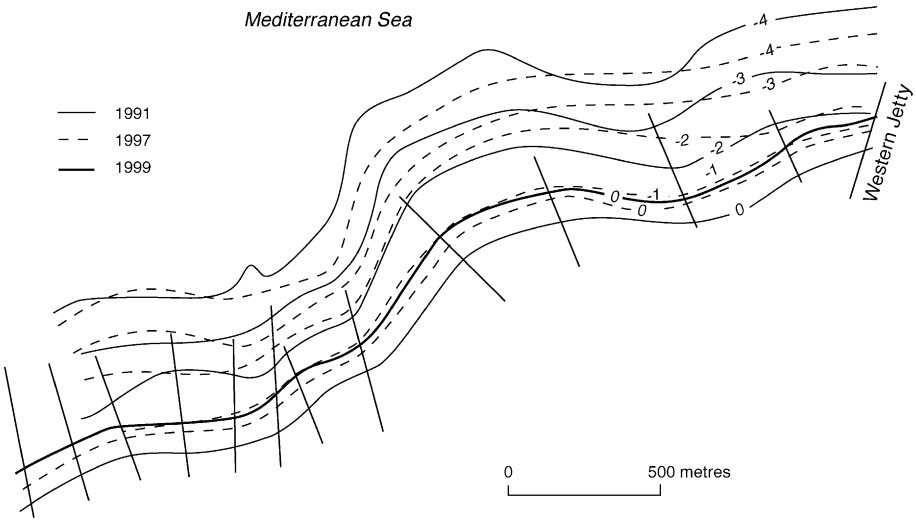

Fig. 3. Bathymetric contours for the accretionary coast west of the harbour showing seaward advance of the shoreline from 1991 to 1999.

the east of the eastern jetty and stated that the effect would be most severe for a distance of 500–1000 m along the shoreline. Our results show that significant amounts of erosion could be detected using our method for some 6.2 km beyond the eastern jetty, towards the coastal resort of Ras El-Bar. It should be noted that, due to the 30 m quantisation of these data, the calculated rates cannot be interpreted as real rates of processes, but they do provide a crude indication of the magnitude of processes and enable detailed field measurements to be seen in a synoptic context. Therefore, coastal modification resulting from the harbour construction would appear to affect some 10.5 km of shoreline in total. Outside this zone, no appreciable change in shoreline position can be determined using the remote sensing methodology adopted here. However, these results indicate that the impact of harbour construction on the Nile Delta shoreline has affected a much larger area than predicted by Sogreah (1982) at the time of construction.

3.1.3. Harbour entrance

An offshore access channel 300 m wide was dredged to permit access to the harbour entrance for shipping. Due to the interruption of longshore sediment transport (Fig. 4), the access channel is experiencing significant silting, particularly near the head of the western jetty. This is due to the summer swell NNE waves and to material passing around the head of the western jetty, and is compounded by material moving down the sides of the access channel, shown by the decreasing slope of the channel sides (Fig. 5). The rate of sedimentation along the access channel is calculated, according to data provided by the Damietta Harbour Authority, to be 1.39×10^6 m^3 year^{-1} prior to 1992. From 1992 to 1995, this rate decreased to 0.8×10^6 m^3 year^{-1}, which is interpreted as indicating relative stabilisation of the channel slopes.

3.2. Sedimentological impacts

A different beach morphology is evident on either side of the harbour. The accretional shoreline to the west of the western jetty is a gently sloping beach. The erosional shoreline to the east of the eastern jetty shows evidence of landward retreat, with significant beach steepening and formation of a small erosional cliff (El-Asmar, 1995). Changes in the sorting processes have resulted in increased concentration of larger discoidal and bladed beach gravels. There is a significant increase in the concentration of opaque and high-density heavy minerals along the beach ripples resulting from erosional removal of lighter minerals.

An investigation was made into the sedimentological impacts of the construction of Damietta Harbour.

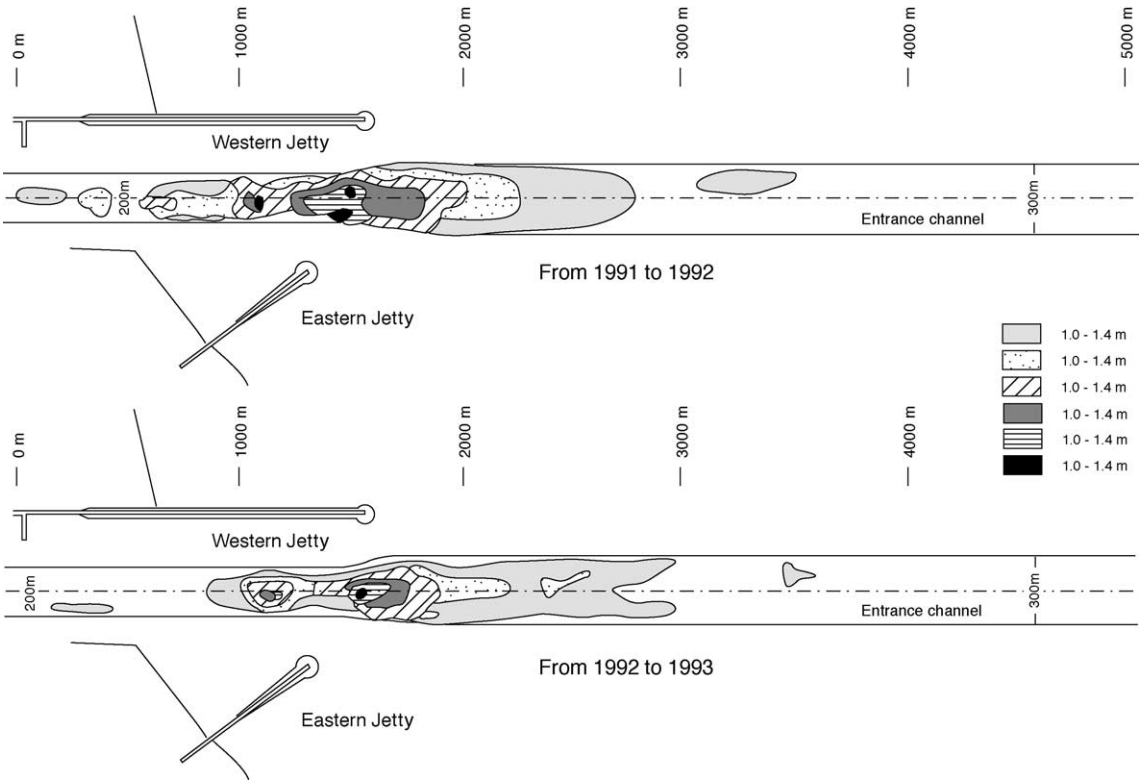

Fig. 4. Map of sedimentation in the access channel. Note that the zero bathymetry is − 15 m (channel depth) and the values given here are the thickness of sediment above zero bathymetry.

To characterise the differences in sedimentological environment on either side of the harbour entrance, 36 beach-face sand samples were collected from either side of the harbour entrance (Fig. 1(b)). These samples were subjected to textural and heavy mineral analyses. Samples from the erosional shoreline to the east of the eastern jetty have significantly different textural parameters. The particle size distributions are unimodal and range between 1.21 and 1.96 ϕ (medium sands) (Fig. 6(a)). The percentage of coarse sand fraction >0.25 mm reaches up to 30% by weight. The samples are all moderately sorted to well-sorted (phi sorting values between 0.80 and 0.49), and symmetrical to very skewed towards the coarser fractions (phi skewness values between − 0.07 and − 0.40). Samples from the accretionary shoreline are characterised by unimodal distributions, with the modal class falling between 2.71 and 3.22 ϕ (fine to very fine sand) (Fig. 6(b)). The percentage of coarse sand >0.25 mm does not exceed 7% by weight of any of the samples. Samples are all moderately sorted to well-sorted (phi sorting values between 0.71 and 0.38), and symmetrical to slightly skewed towards the finer fractions (phi skewness values between 0.01 and 0.11).

Heavy minerals were identified as opaques (magnetite, ilmenite and pyrite), low-density non-opaques (augite, hornblende, epidote) and high-density non-opaques (garnet, zircon, tourmaline, rutile and monazite). There was a significant difference in the percentage of heavy mineral content from samples on either side of the harbour entrance. Samples from the erosional shoreline east of the eastern jetty have values between 10.24% and 93.21% (average 34.42%), with dominance of opaques and high-density heavy minerals (Fig. 6(a)). Samples from the accretionary shoreline west of the western jetty have values between 3.53% and 9.68% (average 5.41%), with dominance of non-

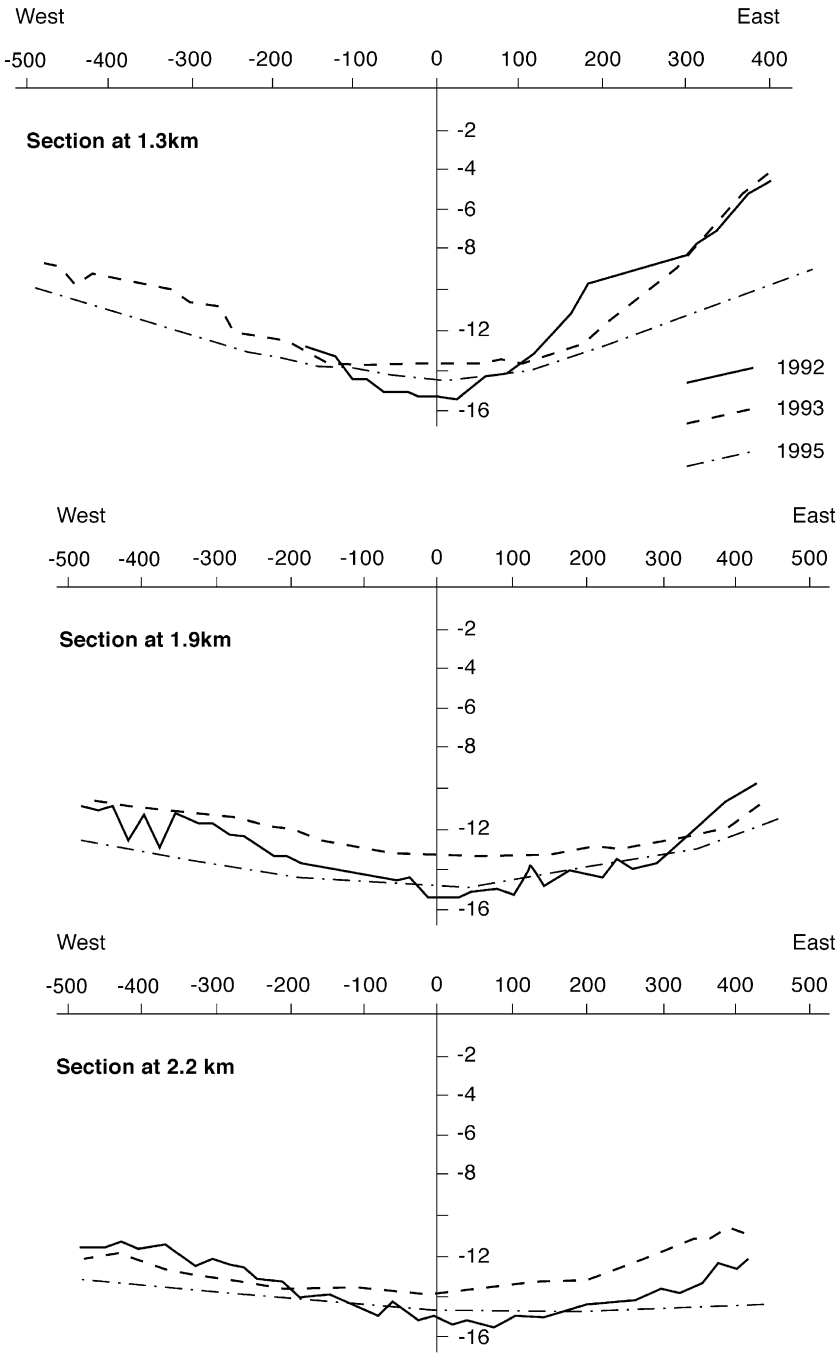

Fig. 5. Bathymetric survey sections along the access channel showing the changes in depth and side inclination.

opaques low-density heavy minerals (Fig. 6(b)). The high variance between samples from east of the eastern jetty results from the high degree of density sorting. These results contradict in part the conclusions of Frihy and Komar (1993), who found that erosional beaches on the Nile Delta are often characterised by

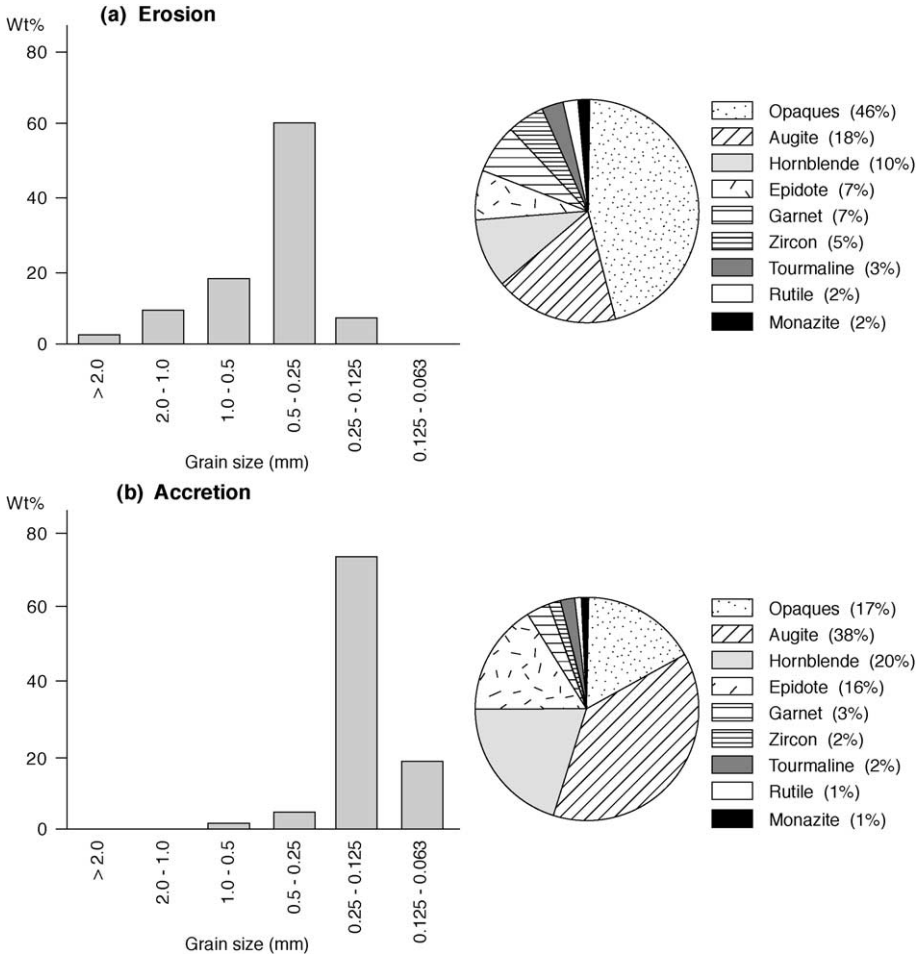

Fig. 6. Grain size and heavy mineral distribution along the (a) western accretional coast and (b) eastern erosional coast of the Damietta Harbour, north of the Nile Delta.

finer sands. However, these workers also found that erosional beaches were enriched in heavy minerals compared to accretionary beaches, as is the case in the present study.

4. Conclusions

The change in both wave and current patterns due to construction of Damietta Harbour appears to be responsible for significant changes in the sediment transport system along this section of the Nile Delta coast and, consequently, a changing pattern of process domains. Using relatively coarse (30-m pixels) remotely sensed data over relatively short (1984–1987–1991) time scales, the areas of erosion and deposition can be determined by applying a segmentation algorithm. The results indicate that 10.5 km of shoreline has been affected by sedimentological changes consequent on harbour construction, which is much more than predicted by Sogreah (1982) at the time of harbour construction. Similar changes are occurring in the nearshore environment, resulting in progradation of the bathymetric contours west of the western jetty and silting up of the harbour access channel.

Beach sediments on either side of the harbour provide a sedimentological record of the changes in

process domain. Sediments from the accretionary beach west of the western jetty have a finer mean grain size with a tendency to poorer sorting skewed to the finer fraction and enriched with assemblage of non-opaques low-density heavy minerals. Sediments from the beach of the erosional shoreline east of the eastern jetty are characterised by coarser mean grain size, a tendency to be better sorting skewed to the coarser fraction and enriched in heavy minerals dominated by opaques and high-density non-opaques.

Acknowledgements

The authors wish to thank the Royal Society, U.K. who funded the remote sensing part of this project and the fellowship visit of the first author. We also thank Mrs. Heather Browning (The University of Reading), who drew the diagrams, the Damietta Harbour Authority who provided us with the bathymetric data used herein and Dr. M. Khalil and Mr. E. Assal, Department of Geology, Damietta Faculty of Science for their help in the field. Comments from Robert G. Dean and Alberto Lamberti enabled considerable improvement to the manuscript.

References

A.S.R.T., 1988. Sedimentation in Damietta Harbour: Final report, Cairo, Egypt, 104 pp.

Chen, P.C., Pavlidis, T., 1979. Segmentation by texture using a co-occurrence matrix and a split-and-merge algorithm. Computer Graphics and Image Processing 10, 172–182.

Cross, A.M., Mason, D.C., Dury, S.J., 1988. Segmentation of remotely-sensed images by a split-and-merge process. International Journal of Remote Sensing 9, 1329–1345.

Eid, F.M., Sharaf El-Din, S.H., El-Din, K.A.A., 1997. Sea level variation along the Suez Canal. Estuarine, Coastal and Shelf Science 44, 613–619.

El-Asmar, H.M., 1995. Impact of protection structures on physical and sedimentary parameters along the Damietta coastal area, Nile Delta, Egypt. Egyptian Journal of Sedimentology 3, 111–124.

El-Asmar, H.M., White, K., 1997. Rapid updating of maps of dynamic coastal landforms by segmentation of Thematic Mapper imagery, example from the Nile Delta, Egypt. Proceedings of 23rd Annual Conference of the Remote Sensing Society, The University of Reading. Remote Sensing Society, Nottingham, pp. 515–520.

El-Fishawi, N., 1994. Relative changes in sea level from tide gauge records at Burrulus, central part of the Nile Delta coast. INQUA MBSS Newsletter 16, 53–61.

Fanos, A.M., 1995. The impact of human activities on the erosion and accretion of the Nile Delta coast. Journal of Coastal Research 11, 821–833.

Fleck, M.M., 1992. Some defects in finite-difference edge finders. IEEE Transactions on Pattern Analysis and Machine Intelligence 14, 337–345.

Forshaw, M.R.B., Haskell, A., Miller, P.F., Stanley, D.J., Townshend, J.R.G., 1983. Spatial resolution of remotely sensed imagery, a review paper. International Journal of Remote Sensing 4, 497–520.

Frihy, O.E., Komar, P.D., 1993. Long-term shoreline changes and concentration of heavy minerals in beach sands of the Nile Delta, Egypt. Marine Geology 115, 253–261.

Frihy, O.E., Fanos, A.M., Khafagy, A., Komar, P.D., 1991. Patterns of nearshore sediment transport along the Nile Delta, Egypt. Coastal Engineering 15, 409–429.

Frouin, R., Schwindling, M., Deschamps, P.Y., 1996. Spectral reflectance of sea foam in the visible and near-infrared. In situ measurements and remote sensing implications. Journal of Geophysical Research 101, 14361–14371.

Kadib, A., 1969. Rate of littoral drift at Ras El-Bar using fluorescent tracers. Suez Canal Authority Research Centre Report, number 42, 1600-1617.

Kettig, R.L., Landgrebe, D.A., 1976. Classification of multispectral image data by extraction and classification of homogeneous objects. IEEE Transactions on Geoscience Electronics 14, 19–26.

Lemoigne, J., Tilton, J.C., 1995. Refining image segmentation by integration of edge and region data. IEEE Transactions on Geoscience and Remote Sensing 33, 605–615.

Lotfy, M., Frihy, O.E., 1993. Sediment balance in the nearshore zone of the Nile Delta coast, Egypt. Journal of Coastal Research 9, 654–662.

Millington, A.C., Townshend, J.R.G., 1987. The potential of satellite remote sensing for geomorphological investigations, an overview. In: Gardiner, V (Ed.), International Geomorphology 1986 Part II. Wiley, Chichester, pp. 331–342.

Nafaa, M.G., 1995. Wave climate along the Nile Delta coast. Journal of Coastal Research 11, 219–229.

Sogreah, M., 1982. Effects on the construction of the Port of Damietta on the evolution of the littoral drift. Consultancy Report, number 35/1202/R9, 35 pp.

Sonka, M., Hlavac, V., Boyle, R., 1993. Image Processing, Analysis and Machine Vision Chapman & Hall, London, 555 pp.

Stanley, D.J., 1996. Nile Delta, extreme case of sediment entrapment on a delta plain and consequent local land loss. Marine Geology 129, 189–195.

Tetra Tech., 1984. Shoreline master plan for the Nile Delta coast. Progress Report number 1, 143 pp.

Townshend, J.R.G., 1980. The Spatial Resolving Power of Earth Resources Satellites: NASA Technical Memorandum 82020. Goddard Space Flight Center, Greenbelt, MD, 36 pp.

Townshend, J.R.G., Cushnie, J., Hardy, J.R., Wilson, A., 1988. Thematic Mapper Data; Characteristics and Use. NERC Scientific Services, Swindon, 55 pp.

UNESCO/UNDP, 1978. Coastal Protection Studies. Final Technical Report, UNESCO, Paris, vol. 1, 155 pp.

Weszka, J., Dyer, C.J., Rosenfield, A., 1976. A comparative study of texture measures for terrain classification. IEEE Transactions on Systems, Man and Cybernetics 3, 610–621.

White, K., El-Asmar, H.M., 1999. Monitoring changing position of the coastline using Thematic Mapper Imagery, an example from the Nile Delta. Geomorphology 29, 93–105.

Wilson, P.A., 1997. Rule-based classification of water in Landsat MSS images using the variance filter. Photogrammetric Engineering and Remote Sensing 63, 485–491.